

# Quantum statistics and anharmonicity in the thermodynamics of spin waves in ferromagnetic metals

Haohua Wen and C. H. Woo\*

*Department of Mechanical Engineering, The Hong Kong Polytechnic University, Hong Kong SAR, China*

(Received 23 March 2016; published 1 September 2016)

The average energy needed to create a magnon is high in ferromagnetic metals due to the high-strength spin stiffness, which results in strong quantization effects that could be important even at thousands of degrees. To take into account quantum statistics at such high temperatures, the associated effects of anharmonicity of the spin vibrations must be taken into account. In addition to the complex nature of such effects, anharmonicity also affects the occupation of the density of state of the vibration states in the context of quantum statistics. Thus, an unoccupied vibration state might become occupied when its spring stiffness is substantially reduced with anharmonicity. Combined effects of quantum statistics and anharmonicity are expected. In this regard, the thermodynamics of ferromagnetic metals are investigated in this paper through the example of bcc iron between 10 and 1400 K. Theoretical analysis and spin-lattice dynamic simulations are performed, through which the physics behind the complex and dramatic temperature dependence of the thermodynamic functions of bcc iron is understood.

DOI: [10.1103/PhysRevE.94.032104](https://doi.org/10.1103/PhysRevE.94.032104)

## I. INTRODUCTION

Vibrational thermodynamics is important to properties of magnetic materials, particularly for high-temperature applications. Yet, dynamic modeling of the coupled spin-lattice system is challenged on the one hand by the strongly amplitude-dependent restoring forces of the spin vibrations, and on the other by the coupling between the spin and lattice vibrations via the exchange interaction. Both issues require treatment of anharmonic effects beyond well-developed methodologies based on the statistical mechanics of harmonic oscillators [1,2].

In most existent calculations, effects due to such complications have to be neglected, limiting their applicability to the low-temperature regime. Thus, Sabiryanov and Jaswal [3] carried out first-principle studies under the static assumption of frozen phonon and frozen magnon within the harmonic approximation in bcc and fcc iron. Körmann and coauthors [4] performed *ab initio* calculations on bcc iron, and estimated the magnetic, electronic, and vibrational contributions to the Helmholtz free energy also within the harmonic approximation. The calculation did not reproduce the characteristic peak of the specific heat at the Curie temperature [5,6]. A more recent study by Lavrentiev *et al.* [7] based on magnetic cluster expansion took the local magnetic order into account. However, the authors were cautious about the accuracy of the calculation near the Curie temperature  $T_C$  because of the improper way anharmonicity of the spin vibrations was treated in the calculation. Besides anharmonicity, the limited sample size and the restricted phase space in these calculations may also distort boundary conditions and frustrate studies in which lattice periodicity is broken, and where long-range interactions, correlated dynamics, critical phenomena, etc., are important.

To address the concerns of anharmonicity and sample size, Ma, Woo, and Dudarev (MWD) [8] initiated the development of large-scale spin-lattice dynamics (SLD) simulations.

Thermodynamics is treated by applying classical statistical mechanics to the anharmonic mechanical system, in a way similar to conventional large-scale molecular dynamics (MD) models [9].

The use of classical statistics where quantization is significant has led to errors of epic consequences no less than the well-known ultraviolet catastrophe in blackbody radiation. In MD simulations where only vibrations of the atoms are involved, the average energy to excite a phonon is  $\sim 30$  meV, and classical statistics is sufficiently accurate above the Debye temperature [10]. However, no matter whether it is based on experimental spin stiffness [11] or on calculated magnon density of states [12], the average energy needed to create a magnon, e.g., in bcc iron, could be an order of magnitude larger. Thus, quantization effects for spin vibrations would be significant even at thousands of degrees and have to be taken into account. Indeed, by comparing the predictions of classical statistics in MWD with the observed behavior of the vibrational thermodynamics of ferromagnetic metals, deep-seated inconsistencies can be discerned. These include nonvanishing heat capacities and divergent entropies at 0 K which violate the third law, as well as the strong temperature dependencies of the internal energy and heat capacity near the Curie temperature.

The need to take into account quantum statistics at such high temperatures, where harmonic approximation is usually inadequate, presents a problem in the modeling and understanding of the thermodynamics of ferromagnetic materials. To ensure the practicality of SLD over a useful temperature range, Woo *et al.* [13] introduced a scheme in which a quantum-statistical description of the anharmonic ferromagnetic canonical ensemble could be formulated. The ability of the quantized SLD (QSLD) scheme to simultaneously deal with anharmonicity and quantum statistics facilitates elucidation of their combined effects. Such understanding is important for the interpretation of high-temperature thermodynamic behavior of ferromagnetic materials.

This paper is organized as described in the following. The theoretical background is described in Sec. II. In Sec. II A, the formulation of QSLD is reviewed. In Sec. II B, within

\*enchwoo@polyu.edu.hk

the perturbative theoretic concept of anharmonic phonons and magnons, effects of anharmonicity and quantum statistics are considered and their interrelation established. Simulation details are presented in Sec. III. In Sec. IV, combined effects of anharmonicity and quantum statistics on the vibrational thermodynamics of bcc iron are presented and discussed by comparing the temperature dependencies of the experimental and calculated enthalpies, heat capacities, and entropies, from various models. The paper is concluded in Sec. V.

## II. THEORETICAL BACKGROUND

### A. Langevin equations of motion for a canonical ferromagnetic crystal

The ferromagnetic metal is modeled as a canonical ensemble of interacting particles and Heisenberg spins thermally embedded in a noisy environment at temperature  $T$ . The corresponding spin-lattice dynamics (SLD) Hamiltonian can be written in the form [13]

$$\mathcal{H}_{SLD} = \sum_n \frac{\mathbf{p}_n^2}{2m_n} + U(\{\mathbf{R}\}) - \frac{1}{2} \sum_{n \neq m} J_{nm}(\{\mathbf{R}\}) \mathbf{S}_n \cdot \mathbf{S}_m + \mathcal{H}_{\text{env}}, \quad (1)$$

where  $m_n$ ,  $\mathbf{p}_n$ , and  $\mathbf{R}_n$ , respectively, are the mass, momentum, and position of the  $n$ th atom, and  $U(\{\mathbf{R}\})$  is the interatomic potential (many-body) corresponding to the lattice configuration  $\{\mathbf{R}\}$ .  $J_{nm}(\{\mathbf{R}\})$  is the exchange interaction function, the magnitude of which governs the interactions between the spins of neighboring atoms  $m$  and  $n$ , i.e., the spin stiffness. Values of  $J_{nm}(\{\mathbf{R}\})$  are mainly determined by the overlapping of wave functions of the  $d$  electrons, which can be deduced from *ab initio* calculations [8].  $\mathbf{S}_n$  is the atomic spin vector (“spins” in the rest of the paper) of the  $n$ th atom arising from the spin polarization of the atoms according to Hund’s rule. It is related to the net magnetic moment by  $\mathbf{M}_n = -g\mu_B \langle \mathbf{S}_n \rangle$ , where  $g$  ( $\approx 2$ ) is the electron  $g$  factor,  $\mu_B$  is the Bohr magneton, and  $\langle \mathbf{S}_n \rangle$  is the time-averaged atomic spin vector.  $\mathcal{H}_{\text{env}}$  describes the action of the environmental noises on the embedded lattice and spin subsystems to maintain thermodynamic equilibrium. We envisage that the environmental noise consists of a sum of extrinsic and intrinsic noises, in which the former is due to thermal fluctuations and the latter due to quantum uncertainty. In addition,  $\mathcal{H}_{\text{env}}$  is also required to enable the exchange of energy and angular momentum, without which conservation of the total angular momentum in  $\mathcal{H}_{SLD}$  prevents full relaxation of the system. Under the noisy action of  $\mathcal{H}_{\text{env}}$ , the equations of motion of spin and lattice in Eq. (1) can be expressed in the form [13] of Langevin equations,

$$\frac{d\mathbf{R}_k}{dt} = \frac{\partial \mathcal{H}_{SLD}}{\partial \mathbf{p}_k} = \frac{\mathbf{p}_k}{m_k}, \quad (2a)$$

$$\frac{d\mathbf{p}_k}{dt} = -\frac{\partial \mathcal{H}_{SLD}}{\partial \mathbf{R}_k} = -\frac{\partial U}{\partial \mathbf{R}_k} + \sum_i \frac{\partial J_{ik}}{\partial \mathbf{R}_k} (\mathbf{S}_i \cdot \mathbf{S}_k) - \frac{\gamma_L}{m_p} \mathbf{p}_k + \mathbf{f}_k(t), \quad (2b)$$

$$\hbar \frac{d\mathbf{S}_k}{dt} = \mathbf{S}_k \times [\mathbf{H}_k + \mathbf{h}_k(t)] - \gamma_S \mathbf{S}_k \times (\mathbf{S}_k \times \mathbf{H}_k), \quad (2c)$$

where  $\hbar$  is the Planck’s constant and  $\mathbf{H}_k = (g\mu_B)^{-1} \sum_i J_{ik}(\{\mathbf{R}_i\}) \mathbf{S}_i$  is the effective exchange field acting on spin  $k$ . The vibrations of spin and lattice are coupled via the exchange interaction  $J_{ij}(\{\mathbf{R}_i\})$ , which is intrinsically anharmonic due to the amplitude-dependent restoring forces that drives the spin vibrations in the Heisenberg Hamiltonian. Following Ref. [13], we assume environmental noise that is Gaussian and that can be represented by frequency-independent delta-correlated random forces  $\mathbf{f}_k(t)$  on atom  $k$  defined by

$$\langle \mathbf{f}_k(t) \rangle = 0 \quad \text{and}$$

$$\langle f_{ni}(t) f_{lj}(t') \rangle = \mu_L(T) \delta_{nl} \delta_{ij} \delta(t - t'), \quad (3a)$$

and random field  $\mathbf{h}_n(t)$  on spin  $n$  defined by

$$\langle \mathbf{h}_n(t) \rangle = 0 \quad \text{and}$$

$$\langle h_{ni}(t) h_{mj}(t') \rangle = \mu_S(T) \delta_{nm} \delta_{ij} \delta(t - t'). \quad (3b)$$

Here  $\mu_L$  and  $\mu_S$  are parameters characterizing the temperature-dependent amplitudes of the random forces and random fields to mimic the action of the noisy environment on the atoms and the spins. Parameters  $\gamma_L$  and  $\gamma_S$  characterize the corresponding dissipative drags on the atoms and the spins due to the random forces. Subscripts  $i$  and  $j$  denote Cartesian components. We also define the fluctuation-dissipation ratios for the lattice system  $\eta_L \equiv \mu_L/2\gamma_L$  and for the spin system  $\eta_S \equiv \mu_S/2\gamma_S$ , respectively.

The equilibrium phase-space probability distribution functions solved from the stochastic equations Eqs. (2a)–(2c) are functions of the fluctuation-dissipation ratios (see Ref. [13]). On the other hand, quantum equations of motion of the corresponding microcanonical lattice-spin system, i.e., without  $\mathcal{H}_{\text{env}}$ , can be obtained in the Heisenberg picture by imposing the appropriate commutation relations between the operators representing the phase-space variables in Eqs. (2a)–(2c). A standard quantum mechanical description of the dynamics of the harmonic crystal can then be derived in terms of phonons and magnons, where the issue of anharmonicity will be considered in the following section. From the corresponding quantum statistics, Woo *et al.* [13] derived expressions for  $\eta_L$  ( $\eta_S$ ), known as quantum fluctuation-dissipation relations (QFDRs), by identifying the equilibrium energies of the canonical and microcanonical representations of the spin-lattice system at temperature  $T$ . Thus,

$$\eta_L(T) = \int_0^\infty \hbar\omega \left[ \frac{1}{e^{\hbar\omega/k_B T} - 1} + \frac{1}{2} \right] g_p(\omega, T) d\omega, \quad (4a)$$

and

$$\eta_S(T) = \int_0^\infty \frac{\hbar\omega}{e^{\hbar\omega/k_B T} - 1} g_m(\omega, T) d\omega. \quad (4b)$$

We note that in Eqs. (4a) and (4b) the fluctuation forces in  $\eta_L$  and  $\eta_S$  are, respectively, mechanical and magnetic in nature, and are determined by different densities of states (DOS) [13],  $g_x(\omega, T) = \frac{4\pi k^2 \Omega}{(2\pi)^3} [\nabla_{\mathbf{k}} \omega(T)]^{-1}$ , where  $g_p$  and  $g_m$  are for the quasiharmonic phonons and magnons, respectively, with  $\Omega$  being the atomic volume.  $\eta_L$  and  $\eta_S$  are explicitly temperature dependent. The DOS can be obtained from experiments, or from first-principle calculations, or by using a simplified model based on the quasiharmonic approximation, as has

been done in Ref. [13]. It is clear that Eqs. (4a) and (4b) reduce to the classical dissipation fluctuation theorem in the classical limit or when temperature is sufficiently high [13], i.e.,  $\hbar\omega \ll k_B T$ . When quantization is important, i.e.,  $\hbar\omega \gg k_B T$ , the fluctuation-dissipation ratios are explicit functionals of the DOS. This is primarily different from the classical theory, in which the neglect of the commutation relations leads to the quenching of all quantization effects. Indeed, the classical theory accepts thermal excitation of all vibration frequencies as equally probable at finite temperatures, and excludes zero-point fluctuations due to quantum uncertainty. In this regard, we envisage that the dissipative drag produced by the noise due to thermal and quantum fluctuations acts in the same way and is simply additive. We note that without the zero-point fluctuations, the vibration energy and the fluctuation-dissipation theorem of the lattice does not tend to the correct classical limit dictated by the equipartition theorem.

In principle, only one of the heat baths is needed to achieve equilibrium at the correct temperature. However, within the present context the only channel through which the necessary heat transfer to attain equilibrium between the spin and lattice systems is the phonon-magnon interaction. In classical physics, thermal excitations of lattice and spin waves are always allowed irrespective of their frequencies, and heat transfer between the spin and lattice systems can occur efficiently for all temperatures. This is different quantum mechanically because of quantization. Having to rely on phonon-magnon interaction for heat transport to and from the lattice system, the spin system basically can only participate in thermodynamic processes involving the lattice via the low-frequency magnons which can interact effectively with the phonons. Unless the system is sufficiently close to the Curie temperature, heat transfer to the spin system would be very inefficient due to the lack of magnons with suitable frequencies. The resulting demand on computation resources due to the extra-long relaxation time and large simulation cell dimension required to produce the low-frequency magnons can become prohibitive. The use of separate heat baths with the same temperature for the lattice and spin systems is a practical way to solve this problem.

### B. Quantum statistics and anharmonicity

Within the quantum mechanical representations of the dynamics of lattice and spin vibrations in terms of phonons and magnons, the anharmonic ferromagnetic crystal Hamiltonian  $\mathcal{H}$  can be formally written as the sum of a harmonic component  $\mathcal{H}_h$  and an anharmonic correction  $\Delta_a \equiv \mathcal{H} - \mathcal{H}_h$ . Represented using the complete orthonormal set of eigenstates  $\{|n, \mathbf{q}\rangle\}$  of  $\mathcal{H}_h$ ,  $\mathcal{H}$  can be represented in matrix form as [13]

$$\begin{aligned} \langle m, \mathbf{q}' | \mathcal{H} | n, \mathbf{q} \rangle &= [(n + n_0)\hbar\omega_0(\mathbf{q}) + \langle n, \mathbf{q} | \Delta_a | n, \mathbf{q} \rangle] \delta_{mn} \delta_{\mathbf{q}\mathbf{q}'} \\ &+ \langle m, \mathbf{q}' | \Delta_a | n, \mathbf{q} \rangle_{m \neq n, \mathbf{q} \neq \mathbf{q}'}, \end{aligned} \quad (5)$$

where the quantum number  $n$  is an integer ( $n = 0, 1, 2, \dots$ ),  $\omega_0(\mathbf{q})$  is the unperturbed phonon (magnon) frequency, and  $\mathbf{q}$  is the wave vector. The ground-state energy  $n_0\hbar\omega_0(\mathbf{q})$  is due to quantum uncertainty. For phonons derived from a particlelike Hamiltonian, we have  $n_0 = 1/2$ . For magnons derived from the Heisenberg Hamiltonian via the Holstein-Primakoff mapping,  $n_0 = 0$  [14]. The off-diagonal elements in

the last term account for the mixing of the phonon (magnon) states induced by anharmonicity. According to Eq. (5), anharmonicity changes the harmonic phonon (magnon) states through (1) spectral-frequency shift, and (2) spectral-line broadening (or lifetime reduction). The former is a first-order perturbation correction, and the latter, second- and higher-order corrections. Eigenstates  $|\varphi_{\mathbf{k}}\rangle$  of  $\mathcal{H}$ , which we may call anharmonic phonons (magnons), can likewise be expanded as a linear combination of the eigenstates  $\{|n, \mathbf{q}\rangle\}$  of  $\mathcal{H}_h$ , i.e.,  $|\varphi_{\mathbf{k}}\rangle = \sum_{n, \mathbf{q}} |n, \mathbf{q}\rangle \langle n, \mathbf{q} | \varphi_{\mathbf{k}} \rangle$ . The expansion coefficients  $\langle n, \mathbf{q} | \varphi_{\mathbf{k}} \rangle$  (functions of  $\Delta_a$ ) constitute the phonon (magnon) spectrum of  $|\varphi_{\mathbf{k}}\rangle$ .

To concentrate on the physics, it is sufficient to only keep the first-order perturbation corrections in the following discussions. The anharmonic Hamiltonian  $\mathcal{H}$  in Eq. (5) can then be put in the diagonal form  $\langle \varphi_{\mathbf{k}} | \mathcal{H} | \varphi_{\mathbf{k}} \rangle = (n + n_0)\hbar\omega_{\mathbf{k}}\delta_{\mathbf{k}\mathbf{k}'}$ , where we have assumed that the perturbative correction is independent of  $n$ . The frequency shifts from  $\omega_0(\mathbf{k})$  to  $\omega_{\mathbf{k}}$  represent the effect of anharmonicity on the phonon (magnon) dispersion relation. From this point on, to simplify nomenclature, by phonons and magnons we imply the states described by  $|\varphi_{\mathbf{k}}\rangle$ , which refer to the experimentally observable anharmonic quantities. We also follow the common practice and define the Hamiltonian  $\mathcal{H}_h$  of our harmonic basis with a spring stiffness based on the “0 K” (ground state) electronic states associated with corresponding (0 K) crystal properties such as elastic modulus, lattice constants, magnetization, etc. We note that in contrast to the temperature-independent harmonic 0 K phonons (magnons), the anharmonic ones in general have temperature-dependent properties.

In the present discussion, anharmonicity is understood in terms of the amplitude-dependent spring stiffness characterizing the vibration. For lattice and spin vibrations, the spring stiffness may generally be assumed to weaken as amplitude increases. This is obvious for the spin vibrations because of the  $\cos\theta$  dependence in the Heisenberg Hamiltonian, and is a reasonable assumption for an anharmonic lattice to undergo positive thermal expansion. The weakened stiffness due to anharmonicity results in a reduced vibration frequency and a DOS shifting towards the lower-frequency side. This is consistent with the experimentally observed softening of the associated dispersion relations with increasing temperature [11]. The anharmonicity-induced downshift of the DOS has important thermodynamic consequences which we will further discuss in the following.

In terms of the Bose-Einstein statistics, quantized lattice and spin vibrations can now be represented. From the grand-canonical partition function the occupation number of the  $\mathbf{k}$ -mode vibration state at temperature  $T$  can be derived in the form of the Planck distribution [15],

$$\langle n_{\mathbf{k}} \rangle_T = \frac{e^{-\hbar\omega_{\mathbf{k}}/k_B T}}{1 - e^{-\hbar\omega_{\mathbf{k}}/k_B T}}. \quad (6)$$

To facilitate discussion, we define the “ignition” temperature of state  $\mathbf{k}$  by  $T_{\mathbf{k}} = \frac{\hbar\omega_{\mathbf{k}}}{k_B}$  from the mean thermal energy required to excite a vibration mode of frequency  $\omega_{\mathbf{k}}$ . It is then clear that high-frequency states have high ignition temperatures and require high temperature for their excitation. In terms of  $T_{\mathbf{k}}$ , Eq. (6) can be rewritten approximately in the

form

$$\langle n_{\mathbf{k}} \rangle_T \approx \begin{cases} \frac{T}{T_{\mathbf{k}}} - \frac{1}{2} & \text{for } T \geq T_{\mathbf{k}} \\ 0 & \text{for } T < T_{\mathbf{k}} \end{cases} \quad (7)$$

Equation (7) simply says that at temperature  $T$ , only states with low ignition temperatures  $T_{\mathbf{k}} \leq T$  are excited. Indeed, the lower the temperature  $T$ , the smaller is the fraction of DOS occupied. As  $T \rightarrow 0$ , the DOS is empty. Using Eq. (7), the mean energy of the state  $\mathbf{k}$  can be written as

$$E_{\mathbf{k}}(T) = \langle n_{\mathbf{k}} + n_0 \rangle_T \hbar \omega_{\mathbf{k}} \\ \approx \begin{cases} k_{\text{B}}T + (n_0 - \frac{1}{2})\hbar\omega_{\mathbf{k}} & \text{for } T \geq T_{\mathbf{k}} \\ n_0\hbar\omega_{\mathbf{k}} & \text{for } T < T_{\mathbf{k}} \end{cases} \quad (8)$$

Summing up contributions from all modes, the total vibration energy at  $T$ , i.e.,  $\langle E \rangle_T = \sum_{\mathbf{k}} (\langle n_{\mathbf{k}} \rangle_T + n_0) \hbar \omega_{\mathbf{k}}$ , may be expressed approximately in the form  $N f_{oc}(T) k_{\text{B}}T + \varepsilon_0$  using Eq. (8), where  $N$  is the total number of modes and  $\varepsilon_0$  the quantum ground-state energy which vanishes in the classical limit  $\hbar \rightarrow 0$ . In terms of the DOS  $g(\omega; T)$ , one may write  $f_{oc}(T) = \int_0^{kT/\hbar} g(\omega; T) d\omega$  to represent the occupied fraction of the DOS (i.e., ignited states) as a monotonic increasing function of  $T$ . It is clear that as  $T \rightarrow \infty$  or  $\hbar \rightarrow 0$  (classical limit)  $f_{oc}(T) \rightarrow 1$  and the DOS is filled. In this case,  $\varepsilon_0$  vanishes and the corresponding total energy in the classical limit is  $\langle E \rangle_T = N k_{\text{B}}T$  which is also derivable from the equipartition theorem. As a result of anharmonicity, the spring stiffness is amplitude dependent and  $\omega_{\mathbf{k}}$  is temperature dependent. In this context, Eqs. (6)–(8) have the same form as those within the quasiharmonic approximation [16]. At the same time, the anharmonicity-induced downshift of the ignition temperatures corresponding to  $\omega_{\mathbf{k}}$  will produce an increase in  $f_{oc}(T)$  with the same effect as increasing  $T$ . The temperature dependence of  $f_{oc}(T)$  and its effect on the vibration energy are entirely quantum in origin, the effects of which also enter other thermodynamic functions, such as the heat capacity, entropy, and free energy due to standard thermodynamic relations.

We have seen from Eqs. (7) and (8) that as temperature or anharmonicity increases,  $f_{oc}(T) \rightarrow 1$  as the DOS is being filled up and the difference between quantum and classical statistics narrows. One may describe this process as *dequantization*, and the resulting change of statistics and thermodynamics of the system as a quantum-classical transition (QCT). The increased occupancy of the DOS during dequantization is directly reflected in the vibrational thermodynamics we are investigating.

According to Eqs. (7) and (8), increasing the occupancy of the DOS can be achieved via two different but nonexclusive routes: (a) thermally induced by increasing temperature  $T$ ; and (b) anharmonicity-induced downshift of the DOS [see discussion following Eq. (5)] leading to the increase of  $f_{oc}(T)$ . We shall distinguish the two mechanisms by referring to (a) as thermal dequantization (TDQ) and (b) as anharmonic dequantization (ADQ). This can be most easily understood following the example of a Debye-type model in which increasing the DOS occupancy can be accomplished via temperature increase by either increasing temperature or reducing the Debye temperature. In both cases, full occupancy is achieved at the Debye temperature.

Due to the relatively low energy of phonon creation, the associated quantum and classical statistics differ only at low temperatures, i.e., below the Debye temperature, where anharmonicity is weak. This means that quantum statistics and anharmonicity are uncoupled, and QCT can only be activated by TDQ. On the other hand, harmonic magnons have high frequencies due to the strong 0 K spring stiffness of the spin vibration. Below the Curie temperature, their occupation of the magnon DOS is heavily suppressed. Without anharmonicity, the spin degrees of freedom simply cannot effectively participate in the thermodynamics of the system below the Curie temperature (see Sec. IV). However, strong anharmonicity arising from the Heisenberg Hamiltonian could produce, via the softened spring stiffness and the resulting frequency downshift, a more fully occupied magnon DOS to allow QCT to occur via ADQ. From the foregoing, one does not seem to be able to escape having to deal with the coupling between quantum statistics and anharmonicity. In this regard, anharmonicity tends to suppress quantum behavior and enhance classical behavior by increasing the occupancy of the DOS. Conversely, quantum statistics reduces the occupancy of phonon (magnon) DOS and weakens anharmonicity by reducing its perturbative contributions [see Eq. (5)].

The foregoing theory is conceptually illustrated with the schematics in Fig. 1. In this figure, the concepts of ignition temperature, TDQ, ADQ, the temperature variation of the occupancy of the DOS and effects due to the interaction between the phonons and magnons are demonstrated. Nevertheless, numerical solution of the Langevin equations of motion in Eqs. (2a)–(2c) in a SLD scheme based on stochastic forces derived based on quantum-statistical mechanics [13] may be more ideal to put the theory to the test. Our results in this regard will be reported in the following sections.

### III. SIMULATION METHODOLOGY

We consider the typical case of ferromagnons in bcc iron. The full set of SLD equations of motion in Eqs. (2a)–(2c) is solved numerically. The nonmagnetic part of the interatomic interaction  $U$  is derived from  $U_{cs}$ , the CS3-33 potential [17],

$$U = U_{cs} - \left( -\frac{1}{2} \sum_{i \neq j} J_{ij} S_i S_j \right), \quad (9)$$

where the ground-state energy of the spin system (the second term on the right-hand side) has been subtracted off. In Eq. (9),  $S_i$  is the magnitude of the  $i$ th spin, which is fixed in our calculation. We note that the interatomic interaction given by CS3-33 [17] is strongly harmonic with an almost temperature-independent phonon DOS. As a result, there is no phonon softening and the bcc lattice remains stable up to 1400 K in the present calculation.

The cubic simulation cell we used has 16000 atoms contained in  $20 \times 20 \times 20$  bcc unit cells, subjected to periodic boundary conditions. The model is designed to have a sufficiently large size to reduce, to a tolerable level, errors due to the missing energy and entropy contributions from the long-wavelength vibration modes, i.e., low-frequency phonons and magnons, caused by the interference of the periodic boundary condition. Increasing the simulation box to

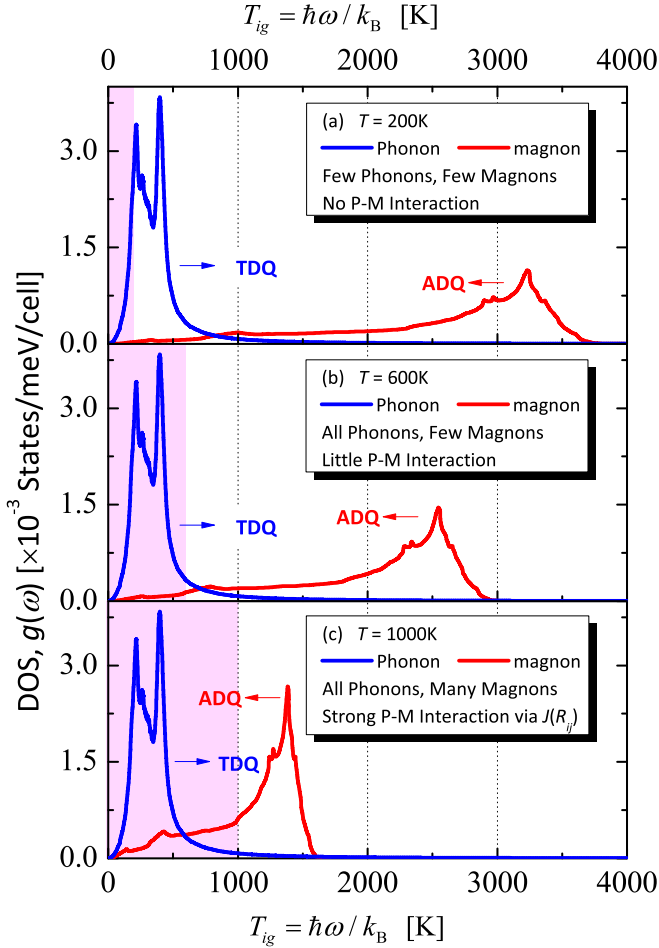


FIG. 1. Illustration of the concepts of ignition temperature, TDQ, ADQ, and occupancy of the DOS, and their relations to temperature dependence of the phonon-magnon (P-M) interaction. The density of states (DOS) of phonon and magnon are shown as a function of the ignition temperature  $T_{ig} = \hbar\omega/k_B$  at various temperatures. The practically temperature-independent phonon DOS is due to the harmonic nature of the lattice potential. In contrast, the strong temperature shift of the magnon DOS is due to the sensitivity of the spin stiffness to the vibration amplitude ( $\cos\theta$ ). The dependence of the DOS occupancy (shaded in red) on ambient temperatures and the related TDQ (phonons) and ADQ (magnons) are noted. (a) At low temperature, e.g., 200 K, there is little phonon and magnon excitation, producing a low specific heat showing little effect of P-M interaction. (b) At medium temperature, e.g., 600 K, all phonon modes are excited, resulting in the saturation of the specific heat due to phonons. Despite the ADQ, the  $T_{ig}$  for magnons is still too high for excitation. The magnon specific heat and effects of P-M interaction are still almost completely suppressed. (c) At high temperature, e.g., 1000 K, all the phonons and the lower-frequency magnons are excited, giving rise to the strong rise in specific heat and effects due to P-M resonant scattering.

54000 atoms or doubling the simulation time produces errors less than 1%. Equilibrations are performed with canonical simulations for a minimum duration of 2 ns with time steps of 1 fs, for various temperatures ranging from 10 to 1400 K. For each temperature, the equilibrium atomic volume is determined by equilibrating the simulation cell under zero

pressure [18]. For QSLD, the Langevin thermostat based on the quantum fluctuation-dissipation relation (QFDR) in Eqs. (4a) and (4b) is employed for temperature control. The phonon and magnon DOS employed in this regard are based on Debye-type quasiharmonic models in which anharmonicity is taken into account [13]. To achieve a stress-free lattice, the dimension length along each direction in the Cartesian coordinate system is sampled using the Berendsen barostat [19] in the sampling time range of 1 ns after equilibrium. The integration algorithm is based on Suzuki-Trotter decomposition [20] which allows parallel computing [21].

For comparison, classical SLD simulations [13] based on classical statistical mechanics, i.e., without accounting for the nonzero commutation relations, and the quantum-harmonic (QH) crystal model (with 0 K phonon and magnon DOS) are also performed. In the latter case, the vibrational energy of the QH model is obtained based on the Debye model [22], where the Debye temperatures used for the phonons and magnons are  $\Theta_D = 430$  K and  $\theta_D = 11\,892$  K, respectively (interested readers are referred to Secs. III and IV of Ref. [13] for details). Standard analytic expressions [16] are used for the calculation of vibrational energy, entropy, and heat capacity. Anharmonic and quantum-statistical effects on the vibrational thermodynamics of bcc iron are evaluated in this comparison.

#### IV. RESULTS AND DISCUSSIONS

Thermodynamic functions, namely, vibrational enthalpies, heat capacities, and entropies, of bcc iron between 10 and 1400 K, are calculated using three models: (1) the standard Debye-type quantum-harmonic (QH) model [16], (2) the quantum SLD (QSLD) model [13], and (3) the classical SLD (CSLD) model [8]. The QH model describes the 0 K noninteracting quantum-harmonic phonons and magnons, the QSLD model describes quantum-statistical anharmonic phonons and magnons, and the CSLD model, anharmonic classical lattice and spin waves. Effects of quantum statistics and anharmonicity on the vibrational thermodynamics are examined by comparing the thermodynamic functions, namely, vibrational energies, heat capacities, and entropies, obtained from the three models. Experimental results [5] are also plotted and compared to aid the analyses.

##### A. The vibrational energy

Vibrational energies from the QH, QSLD, and CSLD models and experimental data [5] are compared in Fig. 2(a). The corresponding spin components are shown in the inset. There is excellent agreement between the experimental data and the QSLD results in which quantum statistics and anharmonicity are simultaneously taken into account. Noted in Fig. 2(a) are (1) the good agreement between the results of both quantum models, QH and QSLD, with the experimental data at low temperatures; (2) the overestimation of the classical result from CSLD compared with the experimental data, reflecting the overexcitation due to the overoccupancy of the DOS in classical statistics; and (3) the underestimation of the QH results at higher temperatures in comparison with the experimental data, signaling errors due to the neglect of anharmonicity. These effects are all anticipated in the general

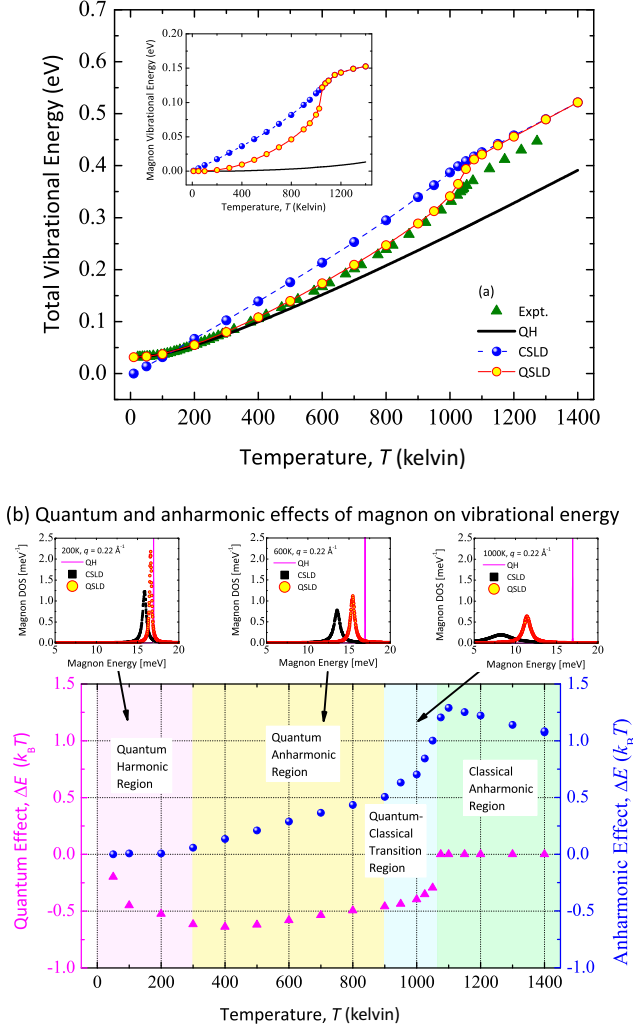


FIG. 2. (a) Total vibrational energies of ferromagnetic bcc iron (involving interacting phonons and magnons) calculated from QH, QSLD, and CSLD models as a function of temperature. Experimental data [5] are plotted for comparison. (b) Correlation of quantum (left label, magenta) and anharmonic effects (right label, blue) on magnon vibrational energy for various temperatures. Insets: magnon energy spectra for wave vector  $q = 0.22 \text{ \AA}^{-1}$  for different models and temperatures (as marked).

theory considered in Sec. II B. Inaccurate interatomic potential for large-amplitude atomic vibrations in the paramagnetic phase above  $\sim 1050 \text{ K}$  may account for the overestimation of the QSLD vibrational energy at these temperatures. In this connection, the instability of the bcc phase due to phonon softening, which leads to the bcc-fcc structural phase transition at  $\sim 1300 \text{ K}$ , is also absent in the present calculation.

As a measurement of anharmonicity of the spin vibrations, the difference between the vibrational energies of the anharmonic (QSLD) and harmonic (QH) magnons are plotted as blue dots in Fig. 2(b). To correlate, we also display in the same figure the effect of quantum statistics (magenta triangles) measured by the difference between the QSLD and CSLD vibration energies. It is clear that both effects are substantial. The vibrational energies due to the three models, from which the blue dots and red triangles are derived, are

TABLE I. Frequency  $\omega^m$ , broadening  $\Gamma^m$ , and lifetime  $\tau^m$  of magnon with wave vector  $q = 0.22 \text{ \AA}^{-1}$  at 200, 600, and 1000 K along the [100] direction in bcc iron, using classical (C) and quantum (Q) fluctuation-dissipation relation.

$T$ (Kelvin)		300	600	1000
$\omega^m$ (meV)	C	15.83	13.55	8.243
	Q	16.58	15.43	11.40
$\Gamma^m$ (meV)	C	0.264	0.431	1.800
	Q	0.151	0.298	0.528
$\tau^m$ (fs)	C	3788	2320	555.6
	Q	6623	3356	1894

shown in the inset in Fig. 2(a). From this figure, it is clear that quantum statistics only allows a limited fraction ( $f_{oc}$ ) of spin vibration states, i.e., the low-frequency ones, to contribute to the thermodynamics of the canonical ensemble. This is consistent with the underestimation of the magnetization in MWD [8] where classical statistics is used.

Blue dots in Fig. 2(b) show close-to-zero anharmonic effects below  $\sim 400 \text{ K}$ , reflecting the harmonic nature of the spin vibrations at low temperatures. Quantum statistics (magenta triangles) corrects the classical vibration energy [see inset in Fig. 2(a)] that has been overestimated due to the excessive occupation of the DOS. The correction is negative and can be seen to remain substantial and shows no sign of letting up until above  $\sim 900 \text{ K}$ . With further temperature increase, Fig. 2(b) sees the QCT in the form of sharp correlated increase in both quantum and anharmonic effects due to ADQ as discussed in Sec. II B. In this connection, the calculated frequency shift and spectral-line broadening of the anharmonic magnons for different temperatures are listed in Table I and shown in the inset magnon spectra for further discussions later in Sec. IV B. From the magnon spectra in the inset the overestimated anharmonic effects in the classical spin waves (CSLD) can also be seen.

## B. The magnon spectrum

Inserted in Fig. 2(b) in various temperature regimes are the spectra of magnons  $|\varphi_q\rangle$  with wave vector  $q = 0.22 \text{ \AA}^{-1}$  for various models calculated for temperatures at 200, 600, and 1000 K. The normalized density of states in the magnon spectra are calculated using the standard approach, i.e., the Fourier transform of the autocorrelation function of spin-vector trajectories [23]. The magenta delta-function-like line corresponds to the 0 K harmonic magnon states calculated from the QH model. The magnon spectra from QSLD is represented by a broadened spectral line outlined by red circles with frequencies downshifted from the magenta unperturbed state. The spectra outlined by black squares represent spin vibrations from the CSLD model. The notably reduced frequency shift and line broadening going from the black (classical statistics) to red (quantum statistics) spectra reflects the reduced occupation in the magnon DOS due to quantum statistics [see Eq. (5)]. Comparing the magnon spectra for increasing anharmonicity as temperature increases, one can recognize the increasing frequency downshifts and line

broadening of the corresponding red and black spectra. The reduction of the frequency shift (from black to red) at 1000 K compared with that at 600 K reflects the increased occupancy of the magnon DOS due to increase of anharmonicity, i.e., ADQ. The physical basis of the correlation between quantum statistics and anharmonicity shown here is as predicted by the theory in Sec. II B. The corresponding numerical values of the mean frequency, spectral-line widths and magnon lifetimes are listed in Table I.

**C. Heat capacity and vibrational entropy**

In Fig. 3(a), we compare the heat capacities calculated from the vibrational energies in Fig. 2(a) by differentiating with respect to temperature. The inset is the spin component of the heat capacity. Consistent with the vibrational energies, there is excellent agreement at low temperatures between the experimental data [5] and both quantum models (QH and

QSLD). We note that the zero heat capacity at 0 K is not only experimentally observed, but also theoretically required. The corresponding classical results based on CSLD in Fig. 3(a) remain at  $4k_B$  at 0 K, consistent with the equipartition theorem. Historically, Einstein was the first to show that this mistake could be corrected by taking into account Planck’s quantization in the formulation of the thermal excitations of the crystal lattice [24].

The rapid increase of the heat capacity at low temperatures reflects the increased occupancy of the phonon DOS during the TDQ of the lattice vibrations which leads to QCT as discussed in Sec. II B. Above  $\sim 400$  K, accuracy of the classical CSLD model starts to improve, but worsens for the QH model. The former is due to the completion of the QCT of the lattice vibrations, and the latter is due to the increasingly anharmonic spin vibrations as temperature increases. The excellent agreement between the QSLD magnons and the experimental result [5] remains intact even beyond 1000 K, successfully reproducing the characteristic sharp rise near the Curie temperature caused by QCT due to the ADQ process as the spring stiffness for spin vibrations softens as discussed in Sec. II B. Without anharmonicity, both the phonons and magnons are noninteracting and the complete absence of the peaking behavior in the harmonic model is expected. On the other hand, the partial suppression of the sharp rise in the classical model is due to the absence of ADQ in a pure classical model in which only the direct effects of anharmonicity, but not its coupling with quantum statistics, are present. We note that the small peak in the CSLD result is due to the coupling between the phonons and magnons.

In Fig. 3(b), quantum-statistical effects (magenta triangles) on the heat capacity of the spins are expressed in terms of the difference between the QSLD magnons and the CSLD spin waves. Corresponding anharmonic effects (blue dots) are measured as the difference between the heat capacities of the QSLD and QH magnons. It is clear from the plots that quantum-statistical and anharmonic effects are highly correlated, as we have discussed in Sec. II B. These results also corroborate those in Secs. IV A and IV B. Increasing temperatures from low to medium causes enhancement of anharmonicity and reduction of quantum-statistical effects, which is shown Fig. 3(b). As temperature increases beyond  $\sim 1000$  K, anharmonicity due to magnon softening increases rapidly, resulting in the sharp downshift of the magnon DOS and its much higher occupancy due to ADQ. This is what leads to the large increase in the heat capacity of the spin component. The highly correlated and very strong anharmonic and quantum-statistical effects are the prominent features of Fig. 3(b), which confirms the significance of the theoretically forecasted ADQ in Sec. II B. Compared with a value of  $1k_B$  for the classical spin heat capacity, the quantum-statistical and anharmonic effects shown in Fig. 3(b) are very significant, if not enormous, particularly near the Curie temperature.

In a related issue, it may be intuitive that short-range magnetic order may still exist in the paramagnetic (PM) phase. However, due to the loss of long-range order, long-wavelength low-frequency ferromagnetic spin waves (magnons) cannot form. On the other hand, the formation of short-wavelength (i.e., high-energy) ferromagnetic magnons need very high thermal energies. Thus, quantum statistics do not favor the

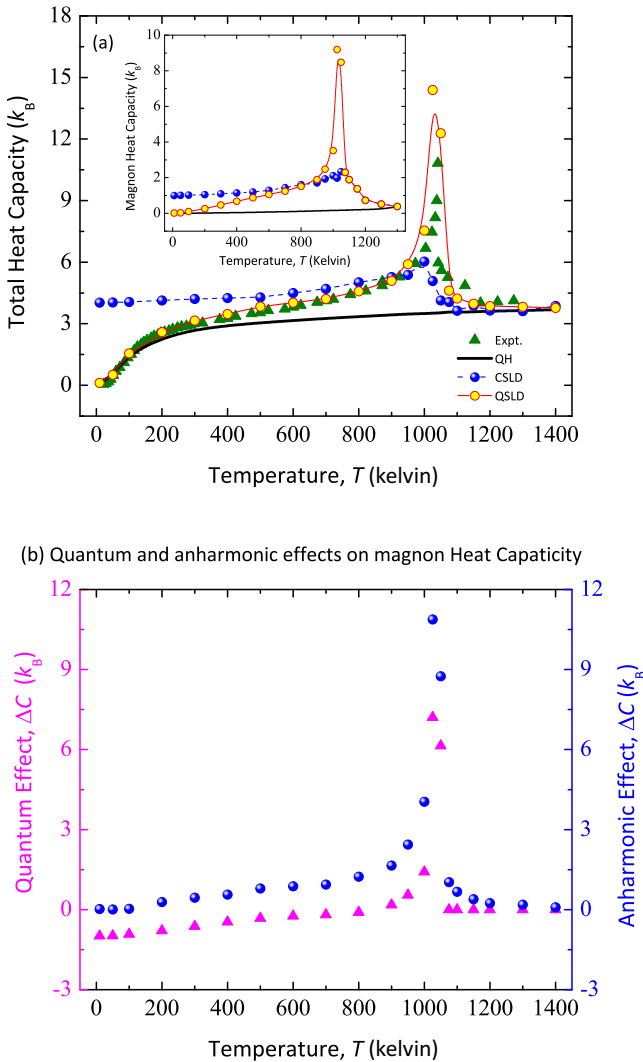


FIG. 3. (a) Total heat capacities of ferromagnetic bcc iron (involving interacting phonons and magnons) calculated from QH, QSLD, and CSLD models as a function of temperature. Experimental data [5] are plotted for comparison. (b) Correlation of quantum (left label, magenta) and anharmonic effects (right label, blue) on magnon heat capacity for various temperatures.

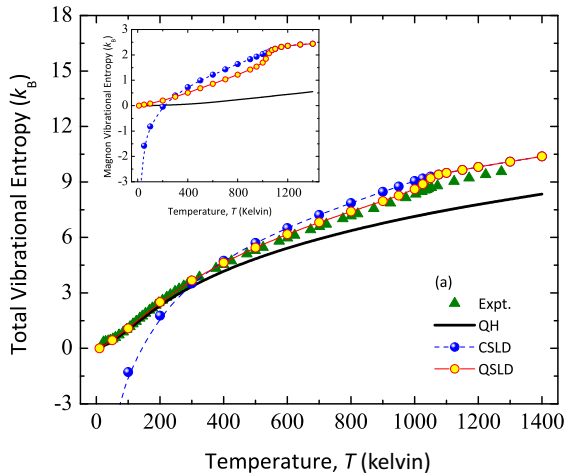
formation of ferromagnetic magnons in the PM phase. This is in contrast with the results of classical dynamics in which the magnon probability distribution is independent of the magnon frequencies [14].

The vibrational entropy  $S(T)$  at temperature  $T$  can now be calculated from the heat capacity  $C_V(T)$  according to the thermodynamic relationship  $S(T) = \int_0^T \frac{C_V(T')}{T'} dT'$ , which satisfies the third law of thermodynamics as long as the integrand is bounded at 0 K [15]. The same procedure cannot be used with the classical statistical theory, because  $C_V(T)$  tends to a constant as  $T \rightarrow 0$ , and the integral diverges as  $\ln(T)$  in this limit. Nevertheless, if the difference between quantum and classical statistics may be assumed to vanish at some temperature  $T_{C+}$  beyond the Curie temperature, one may still obtain the vibrational entropy at  $T$  from the heat capacity by integrating from  $T$  to  $T_{C+}$ . Figure 4(a) shows the vibrational entropies calculated from the heat capacities in Fig. 3(a). Similar to the vibrational energies and heat capacities, agreement

between the two quantum-statistical models, i.e., the QH and QSLD models and the experimental data, is excellent due to the harmonic nature of the lattice and spin dynamics at low temperatures. The quantum results are in marked contrast with the classical results which diverge approaching 0 K, corroborating the gross overestimation of the occupancy of both the phonon and magnon DOS's at low temperatures. With increasing temperature, anharmonic effects increase, particularly for the spin component. Their influence starts to become clearly visible above  $\sim 400$  K. However, the excellent agreement between QSLD and experimental results remains intact to 1400 K.

To obtain a vanishing vibrational entropy at 0 K against the divergent behavior of  $T^{-1}$ ,  $C_V(T)$  has to vanish faster than  $T$ , as  $T$  approaches 0 K [15]. This is a result that cannot be obtained within classical statistics [see Fig. 4(a)]. Beyond the Debye temperature at  $\sim 400$  K, quantum-statistical effects on the phonons disappear due to the thermally induced QCT. Further temperature increase sees the narrowing difference between the quantum (QSLD) and classical (CSLD) anharmonic models of the spin vibrations due to the increase of anharmonicity. Above 1000 K, the narrowing of the difference becomes very conspicuous due to the progression of ADQ. The increase of anharmonicity is also evident in the widening entropy difference between the quantum anharmonic (QSLD) and quantum-harmonic models in Fig. 4(a).

Figure 4(b) concentrates on the magnon contribution to vibrational entropy. The effect of quantum statistics is measured from the difference between the QSLD and CSLD models, and the anharmonic effect from that between the QSLD and the QH models. The prominent feature is the large quantum-statistical effect at low temperatures. This can be traced to the use of the equipartition theorem in the definition of temperature, which is inconsistent with the quantum nature of thermal excitation. The effect of ADQ on the vibrational entropy of the magnons is also clearly shown in Fig. 4(b). Relative to the classical entropy of the spin vibrations which has a value of  $\sim 1k_B$ , both the quantum-statistical and anharmonic effects shown here are very prominent throughout the entire ferromagnetic phase. In this regard, the case of the specific heat is also similar.



(b) Quantum and anharmonic effects on magnon vibrational entropy

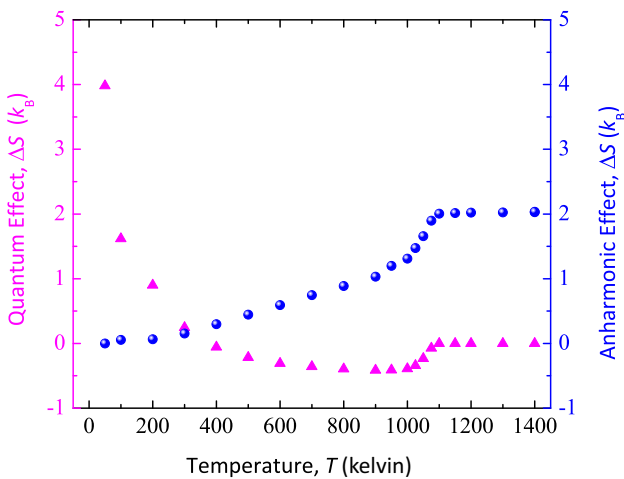


FIG. 4. (a) Total vibrational entropies of ferromagnetic bcc iron (involving interacting phonons and magnons) calculated from QH, QSLD, and CSLD models as a function of temperature. Experimental data [5] are plotted for comparison. (b) Correlation of quantum (left label, magenta) and anharmonic effects (right label, blue) on magnon vibrational entropy for various temperatures.

## V. SUMMARY AND CONCLUSIONS

Given temperature  $T$ , Bose-Einstein statistics basically only allows thermal excitations of vibration modes with ignition temperature  $T_k = \frac{\hbar\omega_k}{k_B} \leq T$ . That  $T_k \rightarrow 0$  for all  $k$  as  $\hbar$  tends to zero means that in the classical limit all existent vibration modes are excited at any nonzero temperature; i.e., all eigenstates of the DOS are filled. Quantum-statistical effects are progressively suppressed with the filling up of the DOS, which can be achieved via two different nonexclusive mechanisms: (a) thermal dequantization (TDQ) by increasing  $T$ , and (b) anharmonic dequantization (ADQ) by downshifting the eigenstates of DOS with increasing anharmonicity (reduction of spring stiffness). A DOS concentrating on low-energy (low-frequency) eigenstates, such as is typical of lattice vibrations (phonons), can be completely filled at low temperatures. Only TDQ is involved in such cases because the anharmonicity of such vibrations is rarely important. On the other hand, with high-energy eigenstates, such as is typical of

magnons representing spin vibrations, complete occupation of the DOS requires high-temperature activation. In such cases, simultaneous operation of both TDQ and ADQ has to be considered.

The foregoing consideration underlies the approach of the present study of the combined effects of quantum statistics and anharmonicity in the vibrational thermodynamics of ferromagnetic metals. Thermodynamic functions, namely, vibrational enthalpies, heat capacities, and entropies, of bcc iron between 10 and 1400 K, are calculated using three models: (1) the QH model describing the 0 K noninteracting quantum-harmonic phonons and magnons, (2) the QSLD model describing quantum-statistical anharmonic phonons and magnons, and (3) the CSLD model describing anharmonic classical lattice and spin waves. Effects of quantum statistics and anharmonicity are examined by comparing the results of the three models among themselves and with experimental results. It is clear that the two effects are coupled and both are important. Detailed analysis allows us to conclude as follows:

(1) Quantum statistics affects all thermodynamic functions, in the form of reduced thermal excitation and heat content relative to the classical counterpart at the same temperature. For lattice vibrations quantum statistics is most significant at temperatures below the Debye temperature, and for spin vibrations, throughout the entire ferromagnetic phase.

Excluding excitation of the high-frequency modes, quantum statistics rectifies the divergent vibrational entropy and restores the vanishing specific heat at 0 K.

(2) As temperature increases, quantum-statistical effects are suppressed as the DOS gets filled. Quantum-classical transition (QCT) induces extra temperature dependence of the vibrational energy, yielding the experimentally observed surges in the specific heat near the Debye and Curie temperatures, which is absent in a classical treatment.

(3) Anharmonicity shifts the DOS towards lower frequencies, thus increasing its occupancy. This reduces the quantum-statistical effects (dequantization), resulting in an increase of the heat content of the sample. Anharmonicity couples with quantum statistics resulting in the enhancement of QCT via ADQ. In the absence of either anharmonicity or quantum statistics, the QCT of the spin vibrations cannot occur, and the sharp peak in the heat capacity of iron due to the spin vibrations would not have existed.

#### ACKNOWLEDGMENTS

This project is initiated and funded by Grant No. 11214114 from the Hong Kong Research Grant Commission, to which the authors are thankful.

- 
- [1] V. P. Antropov, M. I. Katsnelson, B. N. Harmon, M. van Schilfgaarde, and D. Kusnezov, *Phys. Rev. B* **54**, 1019 (1996).
  - [2] D. C. Wallace, *Thermodynamics of Crystals* (Dover, New York, 1998).
  - [3] R. F. Sabiryanov and S. S. Jaswal, *Phys. Rev. Lett.* **83**, 2062 (1999).
  - [4] F. Körmann, A. Dick, B. Grabowski, B. Hallstedt, T. Hickel, and J. Neugebauer, *Phys. Rev. B* **78**, 033102 (2008).
  - [5] D. C. Wallace, P. H. Sidles, and G. C. Danielson, *J. Appl. Phys.* **31**, 168 (1960).
  - [6] Y. S. Touloukian and E. H. Buyco, *Thermophysical Properties of Matter* (IFI/Plenum, New York, Washington, 1970).
  - [7] M. Y. Lavrentiev, D. Nguyen-Manh, and S. L. Dudarev, *Phys. Rev. B* **81**, 184202 (2010).
  - [8] P. W. Ma, C. H. Woo, and S. L. Dudarev, *Phys. Rev. B* **78**, 024434 (2008).
  - [9] D. Frenkel, in *Computer Simulation in Materials Science*, edited by M. Meyer and V. Pontikis (Kluwer, Dordrecht, 1991), p. 85.
  - [10] C. Kittel, *Introduction to Solid State Physics*, 8th ed. (John Wiley & Sons, Inc., New York, 2005), Chap. 5, pp. 105–130.
  - [11] H. A. Mook and R. M. Nicklow, *Phys. Rev. B* **7**, 336 (1973).
  - [12] S. V. Halilov, A. Y. Perlov, P. M. Oppeneer, and H. Eschrig, *Europhys. Lett.* **39**, 91 (1997).
  - [13] C. H. Woo, H. Wen, A. A. Semenov, S. L. Dudarev, and P.-W. Ma, *Phys. Rev. B* **91**, 104306 (2015).
  - [14] D. C. Mattis, *The Theory of Magnetism Made Simple: An Introduction to Physical Concepts and to Some Useful Mathematical Methods* (World Scientific Publishing Co. Pte. Ltd., Singapore, 2006), Chap. 5, p. 175.
  - [15] F. Reif, *Fundamentals of Statistical and Thermal Physics* (McGraw-Hill Book Company, New York, 1965), Chap. 10, p. 404.
  - [16] B. Fultz, *Prog. Mater. Sci.* **55**, 247 (2010).
  - [17] S. Chieas, P. M. Derlet, S. L. Dudarev, and H. Van Swygenhoven, *J. Phys.: Condens. Matter* **23**, 206001 (2011).
  - [18] G. Leibfried and W. Ludwig, *Solid State Phys.* **12**, 275 (1961).
  - [19] H. J. C. Berendsen, J. P. M. Postma, W. F. Van Gunsteren, A. Di Nola, and J. R. Haak, *J. Chem. Phys.* **81**, 3684 (1984).
  - [20] N. Hatano and M. Suzuki, *Lect. Notes Phys.* **679**, 37 (2005).
  - [21] P. W. Ma and C. H. Woo, *Phys. Rev. E* **79**, 046703 (2009).
  - [22] P. Debye, *Ann. Phys.* **39**, 789 (1912).
  - [23] S.-H. Tsai and D. P. Landau, *Comput. Sci. Eng.* **10**, 72 (2008).
  - [24] R. Donald, *Einstein's Other Theory: The Planck-Bose-Einstein Theory of Heat Capacity* (Princeton University Press, Princeton, NJ, 2005), p. 73.